Supporting Information

Compatibility of Lithium Salt and Solvent of Non-aqueous Electrolyte in Li-O_2 Battery

Peng Du, [1¶] *Jun Lu,* [1 ¶] *Kah-Chun Lau,* [2 ¶] *Xiangyi Luo,* [1,5] *Javier Bareño,* [1] *Xiaoyi Zhang,* [3] *Yang Ren,* [3] *Zhengcheng Zhang,** [1] *Larry A. Curtiss,** [2] *Yang-Kook Sun* [4] *and Khalil Amine** [1]

1 Chemical Science and Engineering Division, Argonne National Laboratory, 9700 South Cass Avenue, Lemont, IL 60439, USA

2 Material Science Division, Argonne National Laboratory, 9700 South Cass Avenue, Lemont, IL 60439, USA

3 X-ray Science Division, Advanced Photon Source, Argonne National Laboratory, 9700 South Cass Avenue, Lemont, IL 60439, USA

4 Department of WCU Energy Engineering and Department of Chemical Engineering, Hanyang University, Seoul 133-791, South Korea

5. Department of Metallurgical Engineering, University of Utah, Salt Lake City, UT 84112, USA

¶ *These authors contribute equally.*

Simulation Result:

The hydrophilic feature of LiPF6 from AIMD

Besides using mean square displacement (MSD) to represent the coupled interaction of Li-ion salt and water in the bulk electrolyte, we also compute the radial distribution function (RDF) of several ions species (with and without water presence) to estimate the solvation shell of the ions. During the AIMD simulation, the unique hydrophilic feature of $LiPF_6$ salt in 1NM3 solvent can be seen through the presence of solvated LiF-$(H_2O)PF_5$ or Li+-$(H_2O)PF_6^-$) complex. In contrast to LiPF6, similar close proximity are not found in 1NM3- $LiCF_3SO_3$ which suggests that the fluorinated unit of the triflate ion (i.e. $–CF_3$ group) only interacts weakly with the surrounding H_2O molecules in the electrolyte. To represent this unique dynamic feature qualitatively, the coupling of *Li-O* and *H-F* based on RDF is shown in Fig. S1. As shown in Fig. S1, the solvated average solvated Li^+ with O-site in the 1NM3-LiPF6 is rather sensitive to the presence of water. At the first solvation shells in Fig. S1, the average *Li-O* coordination number ($n_{Li\text{-}O}$) is increase to 2.16 relative to 1.45 when H_2O is present. Whereas in 1NM3- $LiCF_3SO_3$ environment, the change of $n_{Li\text{-}O}$ ~ 3.96 is negligible with respected to the presence of H_2O. Similarly this also found to be case in 1NM3-LiTFSI environment (i.e. $n_{Li\text{-}O}$ ~ 3.99 with and without the presence of H_2O) (Fig. S1). Besides, the strong association of anionic hydration fluorine species of (e.g. $(H_2O)F^-$ or $(H_2O)PF_6^-$) of first solvation shell from $LiPF_6$ is reflected by its significantly larger $g_{H\text{-}F}(r)$ value over the $–CF_3$ group from $LiCF_3SO_3$. From the $g_{H\text{-}F}(r)$, the closest proximity interaction of the F^- ion with the electropositive H-atom of water molecule is within the bond

lengths of ~ 1.7 – 1.9 Å, similar to the reported $(H_2O)_nF^-$ cluster (Ref. 1)

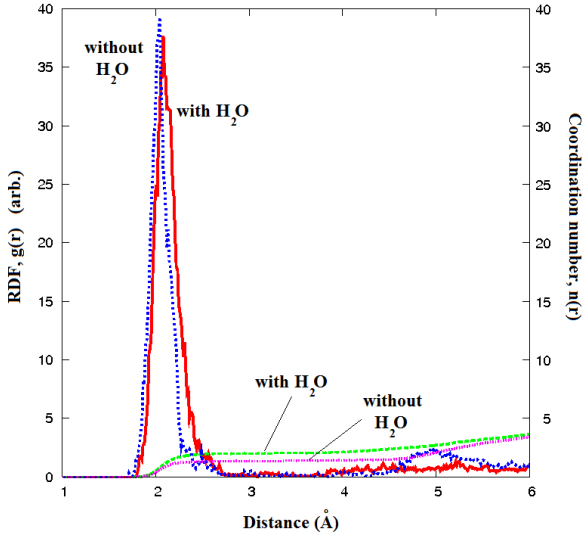

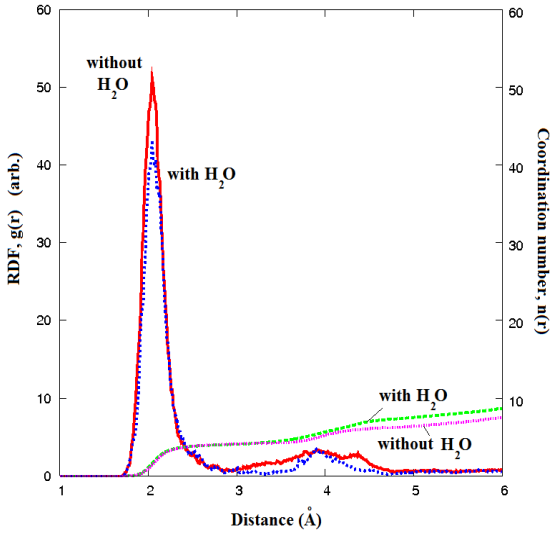

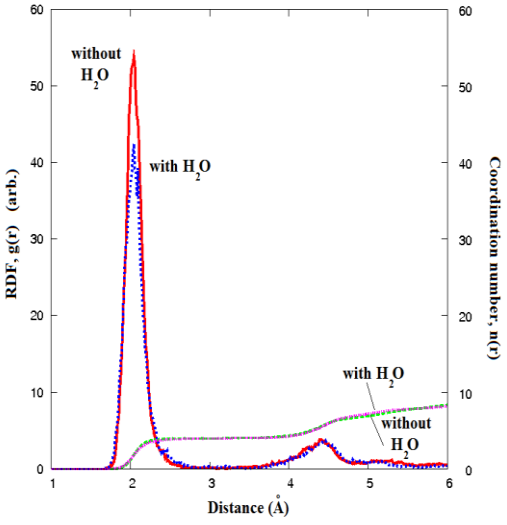

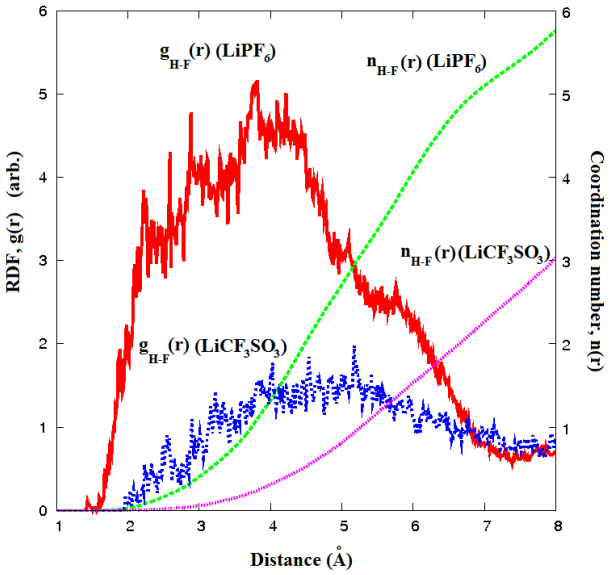

Fig. S1: The Li-O RDF (i.e. $g_{Li\text{-}O}(r)$) and the corresponding average coordination number (i.e. $n_{Li\text{-}O}(r)$) with and without water addition of 1NM3/$LiPF_6$ (top), (center left) 1NM3/$LiCF_3SO_3$ (center right) 1NM3-LiTFSI electrolyte at T = 300 K from 3 ps production run. (Bottom) The *H-F* RDF (i.e. $g_{H\text{-}F}(r)$) and the corresponding average coordination number (i.e. $n_{H\text{-}F}(r)$) among the fluorine and hydrogen atom of water molecules based on these two different electrolytes from the simulation is shown.

The generation of HF through the reaction of Li-salt and H_2O molecule

From the chemical reactions as shown in Fig. S2, it suggests that the generation of HF content in 1NM3-$LiPF_6$ is faster than in 1NM3-LiCF3SO3 and 1NM3-LiTFSI system.

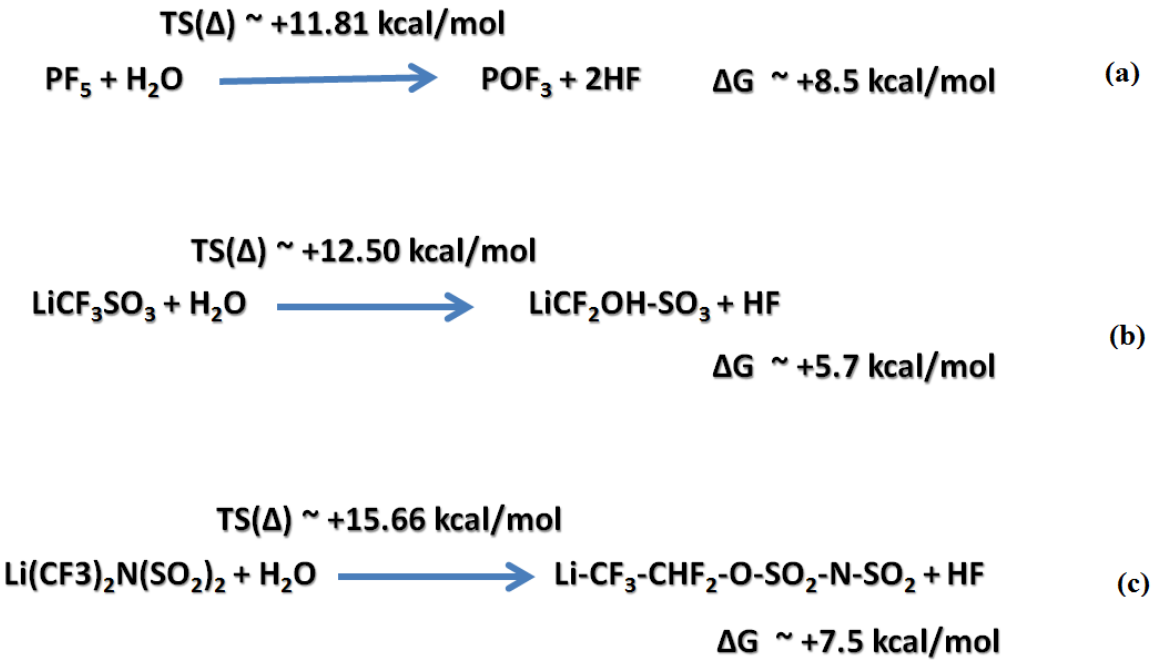

Fig. S2: The chemical reaction between 3 different Li-salt and water computed at T = 298K and 1.0 atm. in 1NM3-solution based on Gaussian09 results: (a) PF_5 (after thermal decomposition of $LiPF_6$ into LiF and PF5) [Ref. 2,3], (b) $LiCF_3SO_3$ and (c) $Li(CF_3)_2N(SO_2)_2$ (or LiTFSI).

The reaction thermochemistry of HF attack against 1NM3 solvent

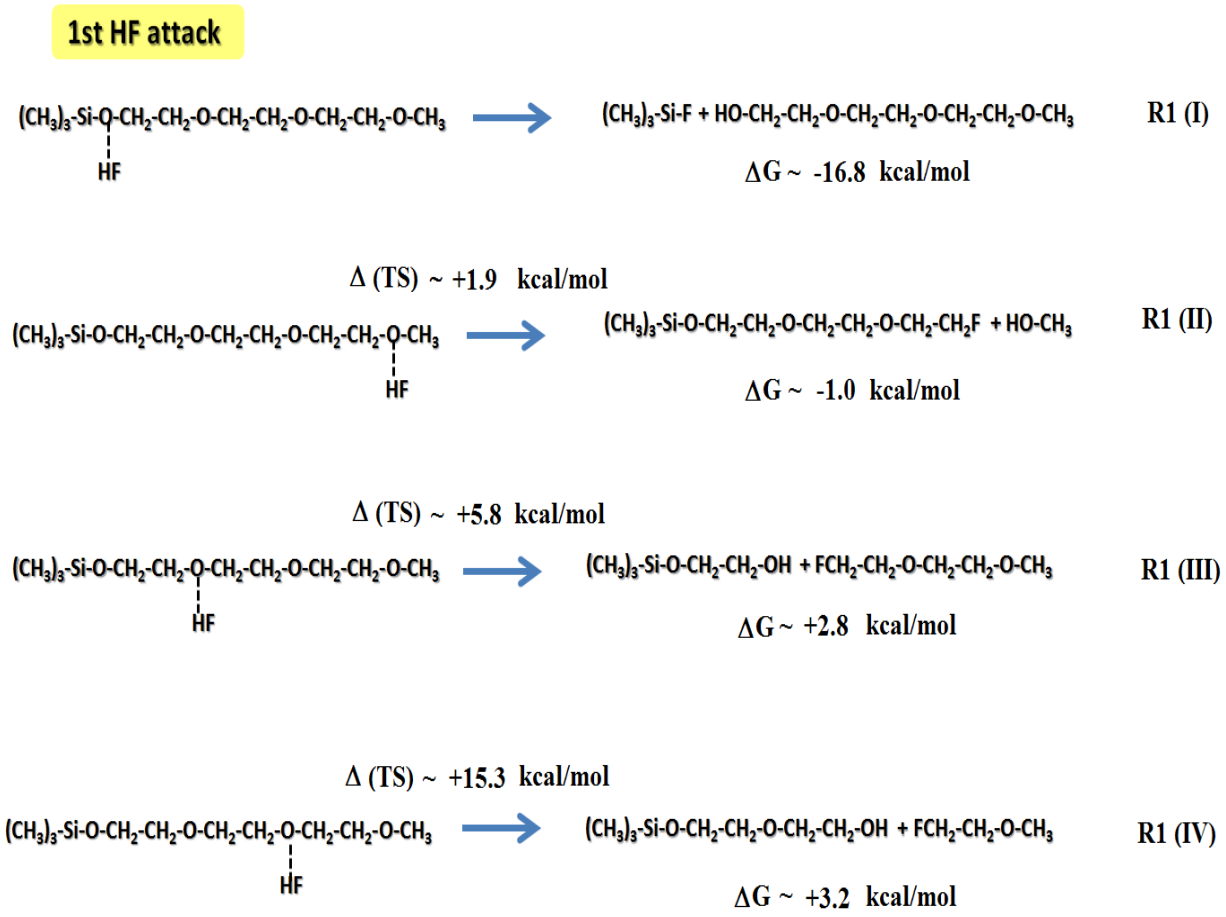

Fig. S3: The possible reaction paths of 1st HF attack against 1NM3 on Si-O bonds (i.e. R1 (I)) and C-O bonds (i.e. R1 (II-IV)). As shown, the R1 (I) reaction path is found to be most favorable with no reaction barrier. The TS(Δ) is the reaction barrier and ΔG is the Gibbs free energy of the reaction in solution with respected to the reactant (i.e. ΔG = 0) at T = 298.15 K and 1.0 atm.

The reaction thermochemistry of HF attack against TEGDME solvent

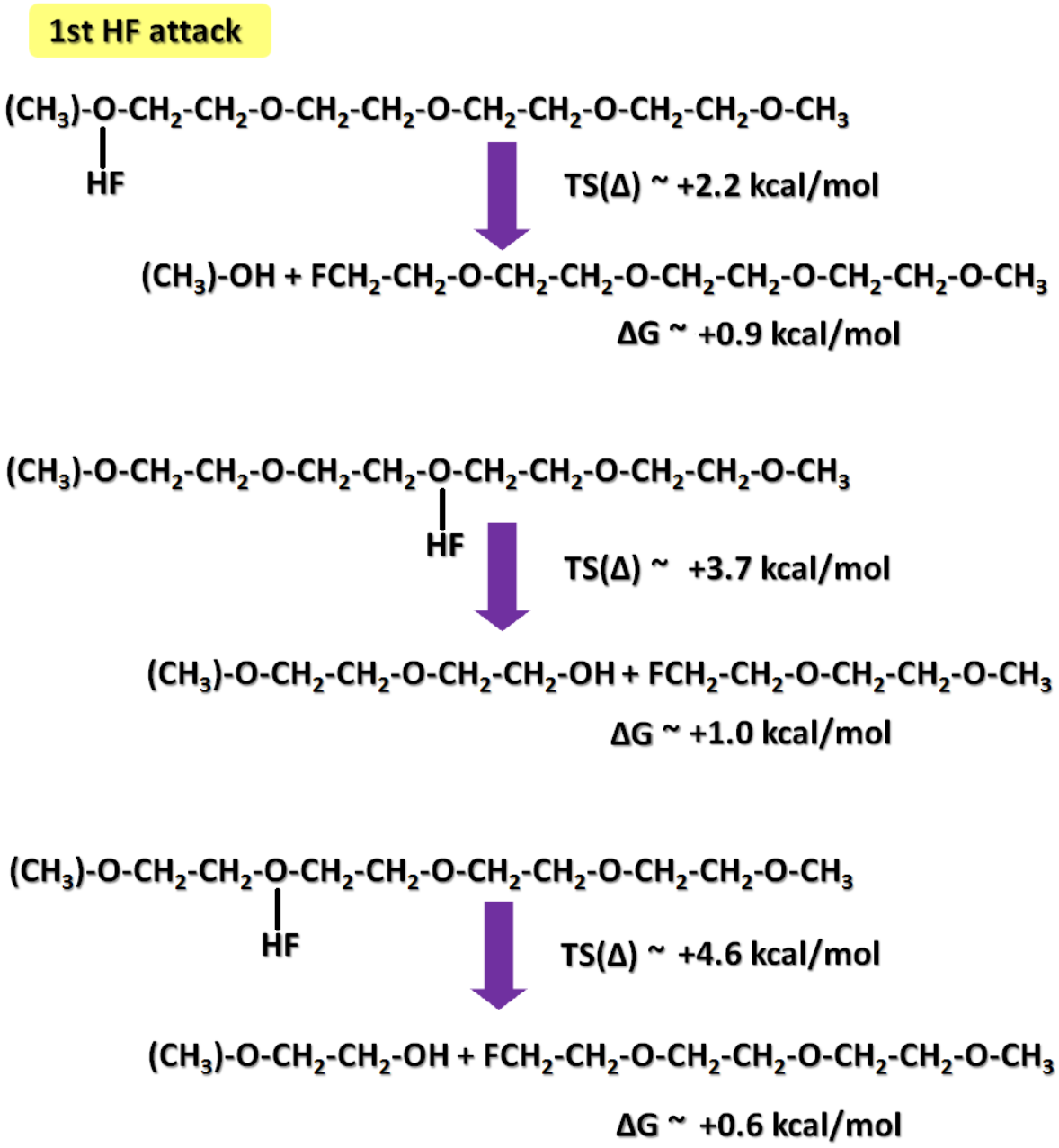

Fig. S4: The possible reaction paths of HF attack against TEGDME on C-O bonds. As shown, all these reactions are found to be endothermic with reaction barrier. The TS(Δ) is the reaction barrier and ΔG is the Gibbs free energy of the reaction in solution with respected to the reactant (i.e. ΔG = 0) at T = 298.15 K and 1.0 atm.

References:

1. S.G. Neogi, P. Chaudhury J. Computational Chemistry, 33, 629-639 (2012).
2. H. Yang, G.V. Zhuang, P.N. Ross Jr. J. Power Source 161, 573-579 (2006).
3. J. Kim, H. Umeda, M. Ohe, S. Yonezawa, M. Takashima, Chem. Lett. 40, 360-361 (2011).